Atom-Based Modeling of Elastic Constants in Amorphous Polystyrene

Tuija Raaska,*,† Satu Niemelä, and Franciska Sundholm

Department of Polymer Chemistry, University of Helsinki, P.O. Box 13 (Meritullinkatu 1A), FIN-00014 Finland

Received February 7, 1994; Revised Manuscript Received July 1, 1994®

ABSTRACT: Molecular mechanics and molecular dynamics simulations have been used to predict the mechanical properties of amorphous polystyrene as a function of the chain tacticity. Relaxed and equilibrated microstructures were generated and the cohesive energy density and the solubility parameter calculated. The amorphous state disorder was analyzed in terms of the pair correlation functions and the Voronoi polyhedra. Two separate methods, the static structure deformation and the stepwise loading molecular dynamics were used to apply small strain deformations to generated microstructures to obtain the elastic constants. The resulting values for moduli are compared, and the performance of the methods is discussed.

Introduction

Molecular modeling provides an opportunity to study the structure of an amorphous polymeric material at the level of individual atoms. By constructing representative microstructures of amorphous polymer and describing the interactions between the atoms by a force field, macroscopically observed behavior of material under stress can be studied. The constructed microstructures are subjected to equilibration and relaxation processes heading toward the mechanical equilibrium state. By deforming the model structures, elastic constants for the bulk material can be estimated within the area of nondestructive forces.

This scheme has been successfully applied to various kinds of polymers in the past: polypropylene,[1-3] polycarbonate of 4,4′-isopropylidenediphenol,[4-6] aromatic polysulfone,[7] poly(vinyl chloride),[8] and poly(1,4-*cis*-butadiene)[9] and poly(1,4-*trans*-butadiene)[10] have been investigated. In their pioneering work Theodorou and Suter[1-3] introduced a method for atomistic simulation of amorphous polymeric glasses. Hutnik, Argon, and Suter[4-6] have studied polycarbonate of 4,4′-isopropylidenediphenol in great detail starting from the generation of force field parameters and the development of the rotational isomeric state model leading to the calculated elastic constants. Fan and Hsu[7] have determined the mechanical and thermal properties of aromatic polysulfone, and Ludovice and Suter[8] extended the method to polar polymers by studying poly(vinyl chloride). Most recent work includes studies on the arrangement of chain segments in amorphous poly(1,4-*cis*-butadiene) by Li and Mattice[9] and poly(1,4-*trans*-butadiene) by Kim, Misra, and Mattice.[10]

Extensions of the simulation technique to more complex polymers have been slow mainly due to the unavailability of force field parameters. The most common way to build up the polymer chain has been Monte Carlo generation,[1-3,9,10] but also RIS (rotational isomeric state) statistics have been used, when available. Various schemes to equilibrate and relax the model structure have been applied. After characterization of the local structure inside the simulation cell, small strain deformations have been applied to estimate the elastic constants. The method developed by Theodorou and Suter[1] is called the static method for estimation of the mechanical properties of amorphous polymeric material. In contrast to this, Brown and Clarke[12] proposed a method based on constant stress molecular dynamics calculation. This method is called dynamic, and although it has been criticized[13,14] due to its disadvantages (time-consuming calculations due to the time scale restrictions, fluctuations of strain with time), we have decided to use it as an alternative way toward the same end.

The main idea in this work is to find the limits of theoretical prediction in estimating mechanical properties, and toward this end two separate methods have been used. Also, it is our intention here to extend the complexity of the polymer chosen for the study. Because the complexity of the backbone has already been increased in previous studies,[4-7] we have tried to extend the side chain. Polystyrene has larger side groups than any polymer studied before. This is the first effort of constructing an amorphous cell where bulky substituents including rings are present. Hence, interactions between the side groups can be studied and the effect of chain tacticity estimated. The unperturbed chain dimensions of polystyrene and its para-substituted derivatives have been investigated theoretically[11] in our group, and RIS models have been developed. It is our intention in the future to study how chain tacticity as well as addition of a small substituent to the para-position of the benzene ring affects the mechanical properties of polystyrene.

Model Construction. Construction of a representative model for amorphous polystyrene is based on the knowledge of the intra- and intermolecular interactions between atoms. The force field acts as an intermediary in the transformation from the microscopic level properties to macroscopic, bulk properties. Despite this, connecting the mechanical performance and structure of polymeric material is a major task. All mechanical properties depend on the crystallinity, orientation, and cross-linking of the material, and it should be emphasized that the model we have built is valid for a totally amorphous, nonoriented or non-cross-linked polymer. In addition, the behavior of the material is assumed to be isotropic.

In an amorphous material there coexist conformations of molecules of similar importance with corresponding terms in the partition function of similar magnitude. Therefore, it is relevant to sample many conformations (to construct an ensemble) to obtain reliable structural information by averaging over the properties.

Polymer chains with a degree of polymerization of 70 were generated using a three-state RIS (rotational isomeric

† Permanent address: Physical Chemistry Division, Department of Chemistry, University of Helsinki.

® Abstract published in *Advance ACS Abstracts,* August 15, 1994.

0024-9297/94/2227-5751$04.50/0

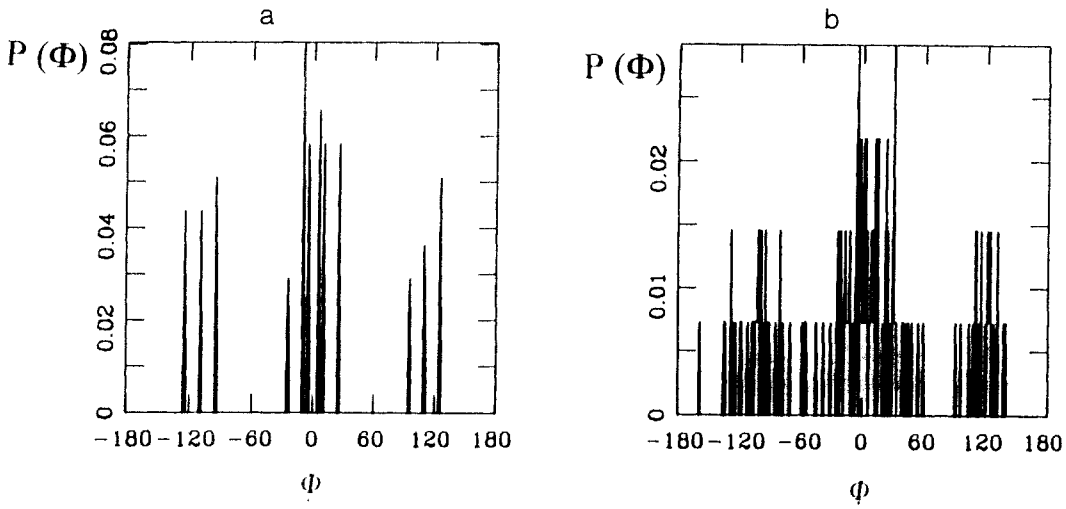

Figure 1. Example of the distributions of the conformational states of backbone dihedral angles (for atactic polystyrene, the probability of occurrence of meso diads being 0.4): (a) before the refinement; (b) after the refinement procedure.

state) model.[11,13] Assigning the conformational states of backbone dihedral angles using the RIS statistical weights results in a chain where the distribution of rotational states is correct. The tacticity of the chain was considered by generating various kinds of chains, isotactic, syndiotactic, and four different atactic chains were constructed. Atacticity was defined by the probability of the occurrence of meso diads in the chain. Hence, the effect of the chain tacticity on the resulting mechanical properties can be analyzed.

For all different tacticities, several chains were created to be able to average over the calculated properties. The chains were built stepwise, placing three-bond sections of the backbone at each step. The quality of the generated structures was improved during the construction procedure by allowing the use of three substates. The width of the substates was 30 degrees. A ring checking algorithm was utilized to prevent the catenation. The chain was packed into a cubic cell using experimental density 1.05 g/cm^3 at temperature 298 K. The resulting edge length of the amorphous cell was 22.59 Å, and the cell included 1122 atoms. The constructed model structures had a high potential energy, and the cell was not homogeneously filled.

Structure Refinement. Commonly applied structure refinement schemes include an alternating molecular mechanics and molecular dynamics simulation using a canonical ensemble. If only a straightforward molecular mechanics minimization were applied, the structure achieved might be the nearest local energy configuration and the system might be trapped into it. In order to find the area in a rough energy hypersurface where the other local minima are located (maybe separated from the other minima by a very low energy barrier), Li and Mattice[9] suggested a different approach. The temperature of the system is increased as high as 800 K for the initial equilibration period where a short duraction (4 ps) NVT molecular dynamics is run. The experimentally impossible temperature is used to achieve a high energy state over the local minima and the barriers between them.

In our work, we utilize the approach by Li and Mattice in the refinement procedure. The initial high energy structures were relaxed by combined molecular mechanics minimization and molecular dynamics simulation. The cell shape is kept fixed during the procedure. A potential cutoff of 8.5 Å was used to increase the speed of calculation of nonbonded interactions. Coarse refinement of the cells included steepest decents minimization until the energy derivatives were less than 5 kcal/mol. This was done to remove all partial overlaps of atoms or charge groups. To equilibrate the system at 298 K, 2000–4000 steps (2–4 ps) of NVT dynamics were carried out using a standard Verlet algorithm. The coarse refinement run ended up with conjugate gradients minimization where the convergence criteria used was 0.01 kcal/mol. After that, the temperature of the system was increased to 800 K and 4000 steps of NVT dynamics were run. This was followed by conjugate gradients minimization until the energy derivatives were less than 0.005 kcal/mol.

Amorphous State. The final relaxed structures were analyzed in order to estimate the efficiency of the refinement procedure and to study the internal structure of the constructed model cell. Distributions of the conformational states of the backbone dihedral angles were compared before and after the refinement procedure (see Figure 1). Notably, the distribution shows clearly the change from the initial three-state RIS model to a more evenly distributed one but which is still obeying the three-state model. The amorphous state order (or disorder) is presented figuratively by pair correlation functions and by numerical values for the cohesive energy density and solubility parameter. The distribution of free volume in the simulation cube was studied in terms of Voronoi polyhedra. Finally, the refined cells were subjected to external load in order to calculate the elastic constants of the material.

Pair Correlation Functions. Pair correlation functions are used in macromolecule simulations to give the probabilities of finding a pair of atoms a distance r apart relative to the probabilities expected for a completely random distribution at the same density.[14] Pair correlation functions are calculated for various pairs of atoms for three types of contributions: total, intermolecular, and intramolecular. For our structures of polystyrenes there are three distinct atom pairs: carbon–carbon, carbon–hydrogen, and hydrogen–hydrogen. The results are collected in Figure 2.

Cohesive Energy Densities and Solubility Parameters. A direct measure for the validity of the relaxed structures is the cohesive energy density and, related to it, the solubility parameter. In atomistic simulations for polymeric materials the cohesive energy is defined as the increase in energy per mole of a material when all intermolecular forces are eliminated. The cohesive energy density is the energy required to break all intermolecular physical links in a unit volume of material. The energy with periodic boundary conditions is calculated first, and

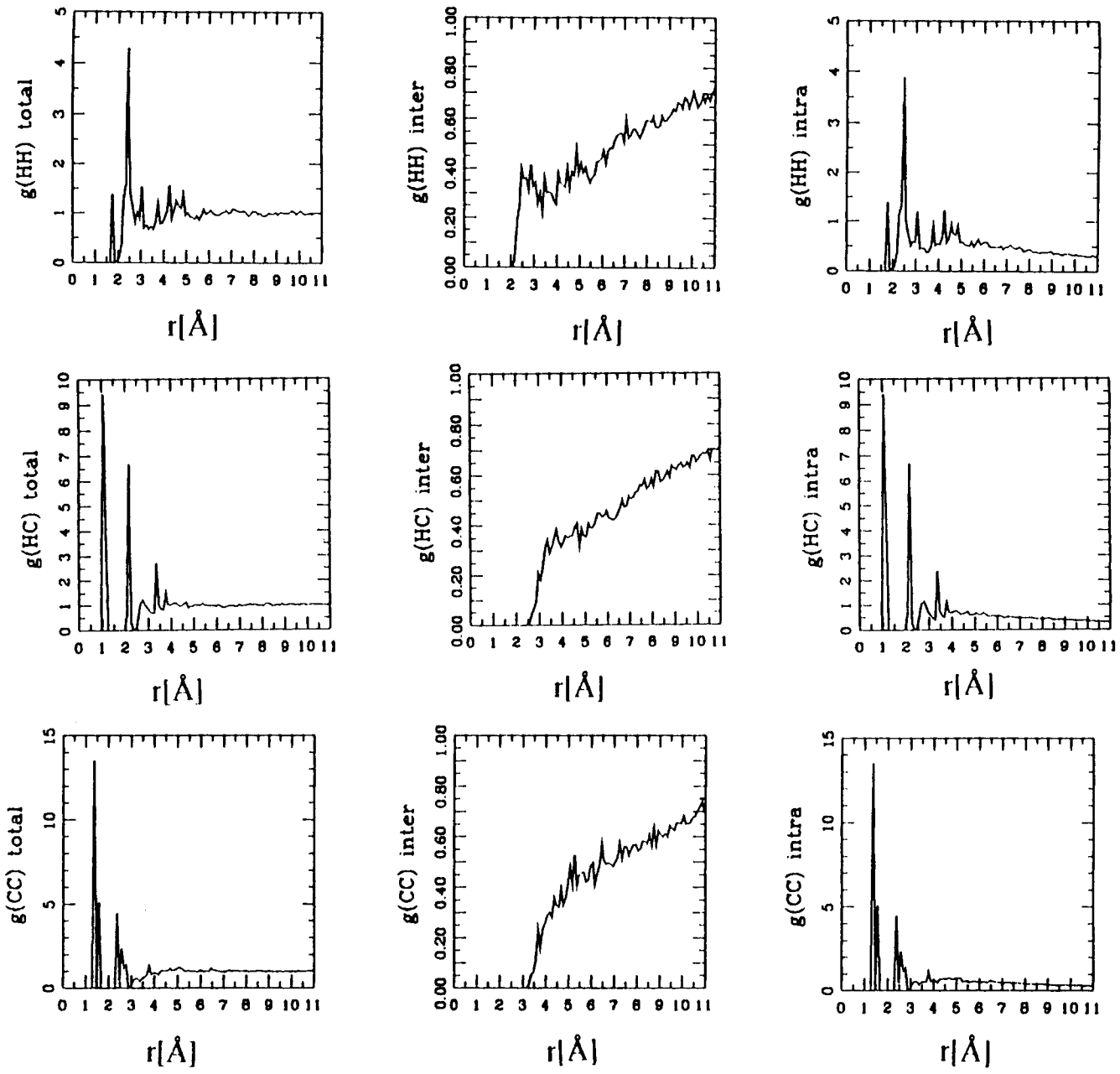

Figure 2. Example of the calculated pair correlation functions, for atactic polystyrene (the probability of occurrence of meso diads being 0.4).

this value is subtracted from the energy calculated for the parent chain when periodic boundary conditions are removed. This calculation is in error due to the use of the cutoff distance, a truncation of the nonbonded potential energy function. This is corrected using a tail correction for the van der Waals energy:

$$U_{coh} = U_{parent} - U_{tot} = U_{parent} - (U_{calc} - \Delta U_{tail})$$

where U_{parent} denotes the intramolecular energy of the parent molecule, U_{calc} is the energy given by the simulation using the potential cutoffs, and ΔU_{tail} is the tail correction. Formulation for the tail correction calculation has been published elsewhere.[1,8]

An experimentally measurable quantity, the Hildebrand solubility parameter, is defined[8] as the square root of the cohesive energy density:

$$\delta = (U_{coh}/V)^{1/2}$$

The solubility parameter quantifies the interactions between the polymer and the solvent. Typically, atom-based modeling yields predictions for this parameter which are typically lower than the experimental values (see refs 1–10).

Free Volume Probing by Voronoi Tessellation Statistics. Free volume distribution in the generated amorphous microstructures is defined by Voronoi tessellations or Voronoi polyhedra. Voronoi polyhedra are analogues to the Wigner–Seitz cells in solid-state physics: the Voronoi polyhedron is the smallest convex polyhedron restricted by the planes that perpendicularly bisect the straight lines that connect one atom to the other. The polyhedron encloses all the space that is nearer to the central atom than any other atom. Disordered systems (like an amorphous polymer) generate a distribution of polyhedra with various shapes and sizes. The statistical distribution of quantities such as polyhedron volumes, surface areas, reduced surface/volume ratio, and the number of faces per polyhedron constitutes the description of the amorphous state structure. As a Voronoi polyhedron around an atom identifies the available space of its own,

Table 1. Energies of Corresponding Five Relaxed Structures (kcal/mol) for Atactic Polystyrene (Probability of Occurrence of Meso Diads 0.4)

polystyrene	structure 1	structure 2	structure 3	structure 4	structure 5	deviation
total	-43.2	-44.4	-62.4	-59.5	-45.0	-50.9 ± 8.2
stretching	170.8	166.0	169.7	162.6	167.5	167.3 ± 4.1
bonding	239.6	186.3	211.3	188.5	215.4	208.2 ± 26.7
torsion	-476.8	-451.4	-478.0	-479.6	-474.5	472.2 ± 14.1
nonbond	208.2	224.0	214.2	225.5	208.7	216.1 ± 8.7
repulsion	3443	3487	3445	3458	3447	3456 ± 22
dispersion	-3235	-3263	-3231	-3252	-3239	-3244 ± 14
coulombic	-11.7	-11.0	-15.6	-4.8	-9.3	-10.5 ± 3.5

Table 2. Cohesive Energy Densities and Solubility Parameters for Polystyrene

polystyrene	probability of occurrence of meso diads	cohesive energy density, $\times 10^{-7}$ (cal/m^3)	solubility parameter, (cal/cm^3)$^{1/2}$
syndiotactic	0.0	6.5 ± 0.2	8.1 ± 1.4
atactic	0.2	5.9 ± 0.3	7.7 ± 1.7
atactic	0.4	5.6 ± 0.3	7.5 ± 1.7
atactic	0.6	5.4 ± 0.3	7.3 ± 1.7
atactic	0.8	5.0 ± 0.4	7.1 ± 2.0
isotactic	1.0	4.7 ± 0.2	6.9 ± 1.4
exptl value,[21] atactic			8.0–10.6

this information can be related to the free volume or void volume in dense, amorphous polymers.

Estimation of Mechanical Properties. When an ensemble of microscopic structures is constructed and mechnical equilibrium achieved, calculation of the elastic constants associated with an amorphous polymer can be performed utilizing several methods. Detailed formulation of the methods has been given elsewhere;[1-3,12] only main features are concluded here. It should be noted that the cubic shape of the motif simplifies the calculations drastically.

Elastic Constants by Static Structure Deformation. The static method introduced by Theodorou and Suter[1] resorted on two basic assumptions: contributions that might originate from changes in configurational entropy on deformation and those from the strain dependence of the vibrational frequencies were considered negligible. Also, bond lengths and bond angles were kept constant; only torsional angles were allowed to change in minimizations. In their method a unidirectional external load is applied to the cell and the energy of the structure is minimized under constant stress. The elastic constants are calculated from the ratio of the applied stress to the change in the cell size. The first derivative of the potential energy with respect to strain is the internal stress tensor σ, and the second derivative represents the stiffness matrix. Elastic properties of the material are completely described by the stiffness matrix. The stiffness matrix is calculated in the following way:

$$C_{ij} = \frac{1}{V}\frac{\partial^2 U}{\partial \epsilon_i \partial \epsilon_j} = \frac{\partial \sigma_i}{\partial \epsilon_j} = \frac{(\sigma_{i+} - \sigma_{i-})}{2\epsilon_j}$$

where U is the total energy, V is the volume, and ϵ_i and ϵ_j components i and j of the strain tensor. σ_{i+} and σ_{i-} are the components associated with the stress tensor under tension and compression, respectively.

In the limit of zero strain the stiffness matrix reduces to a single 6 × 6 second rank tensor which for an amorphous, isotropic material includes only two independent coefficients. These coefficients λ and μ (also called Lame's constants) are required to specify the elastic behavior. More commonly applied constants, Young's modulus E, Poisson's ratio ν, bulk modulus B, and shear modulus G can be obtained from Lame's constants.[2]

Elastic Constants from a Stepwise Loading Molecular Dynamics Method. The loose coupling constant pressure molecular dynamics method is an alternative way of calculating elastic constants. The static model described in the previous section does not include the entropic effects. On the contrary, the entropy contribution is implicitly included in the dynamic method. This method has been proposed by Berendsen,[15] and it has been adapted and extended for use on polymer samples by Brown and Clarke.[12] In this method, elastic constants are described by the response of the pressure tensor to strain. The pressure changes are accomplished by changing the coordinates of the atoms. The size as well as the shape of the simulation cell with periodic boundary conditions is allowed to vary: the microstructure adjusts to the imbalances between an externally applied tensorial pressure and internally measured pressure tensor. The pressure imbalance is coupled to the first derivative of the basis vectors. The first derivative gives the usual pressure tensor; the second derivative produces averages of fluctuation of pressure tensor components. These so-called fluctuation terms arise from the changes in the relative probability of the system's states brought about by the deformation itself. This kind of coupling reduces the tendency to unphysical oscillatory response: in fact the motions of the cell are overdamped. Brown and Clarke[12] have shown that it is also possible to model yielding by using their method. However, their work does not refer to any specific polymer (although their model resembles polyethylene), and hence comparison to experimental values cannot be made.

Computational Details

Molecular Mechanics Calculations. The molecular mechanics and molecular dynamics calculations performed in this work were carried out using DISCOVER software package by Biosym Technologies Inc.[16] The force field used is the CFF91 force field published by Maple, Dinur, and Hagler[17] and implemented in DISCOVER module of the BIOSYM software. CFF91 is a second generation, class II, force field which employs a quadratic polynomial for bond stretching and angle bending. The torsional potential has a form of a three-term Fourier expansion. For out-of-plane coordinates a Wilson definition is used which is based on the angle between the actual bond and its projection onto the plane of the other three atoms. A Lennard-Jones (6–9) potential was selected to describe the van der Waals interactions and a Coulombic potential to represent the electrostatic interactions. Various kinds of off-diagonal terms representing couplings between deformations of internal coordinates have been inserted (for details, see ref 19). This force field is in continuous development.[18,20]

Amorphous cell constructions as well as graphics were performed using a Silicon Graphics Personal Iris 4D/30

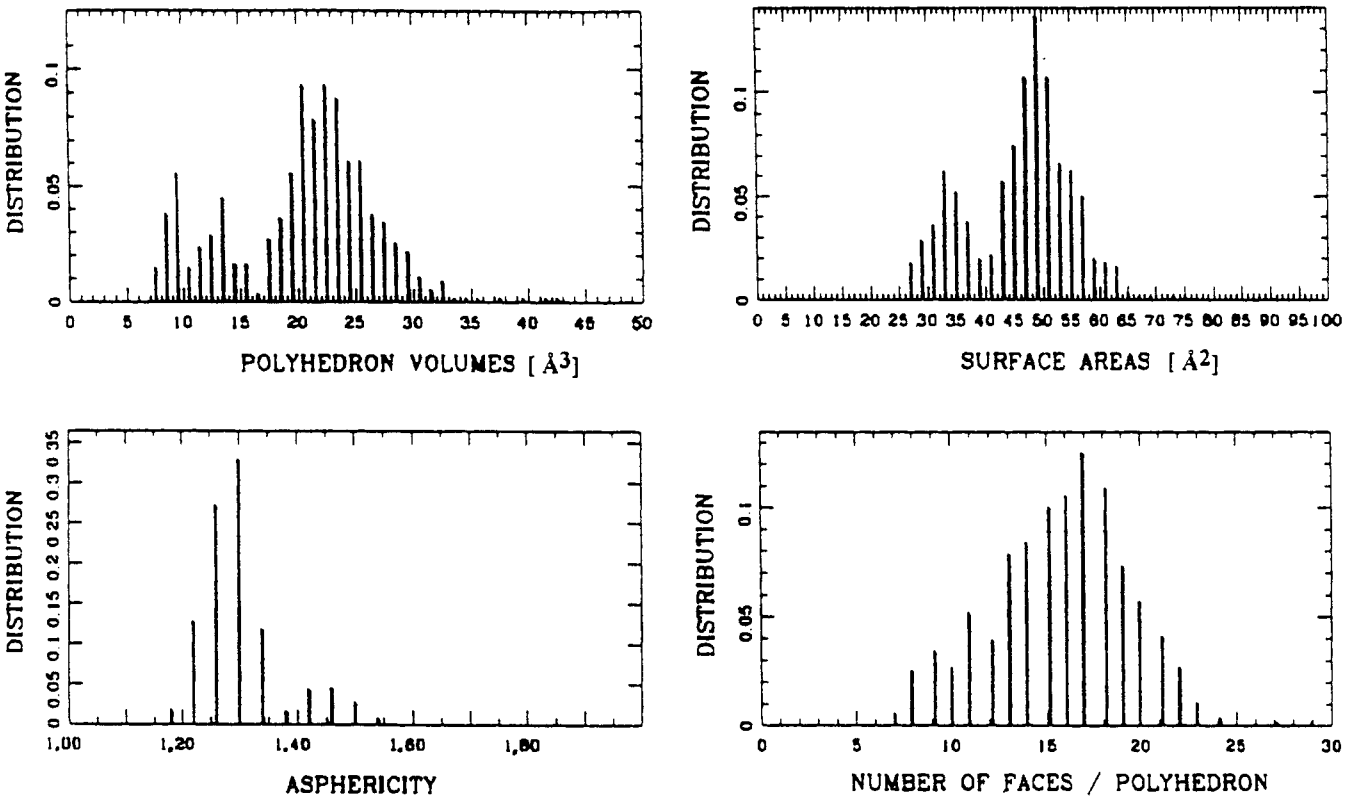

Figure 3. Example of a typical distribution of Voronoi polyhedra for carbon atoms for atactic polystyrene (the probability of occurrence of meso diads being 0.4). Distributions of polyhedron volumes, surface areas, and number of faces per polyhedron are given. The distribution of the reduced surface per volume ratio, which is a measure for the asphericity of a polyhedron, is also plotted.

Table 3. Volume Distribution of Voronoi Polyhedra for Carbon Atoms as a Function of Chain Tacticity

	probability of occurrence of meso diads, %					
	0.0	0.2	0.4	0.6	0.8	1.0
volume/Å^3						
<20	41	40	38	40	39	38
20–25	44	42	43	40	40	40
>25	15	18	19	20	21	22

workstation. Molecular mechanics and molecular dynamics simulations were performed using an Iris 4D/380 VGX workstation and the Cray X-MP EA/432 supercomputer at the Centre for Scientific Computing (Espoo, Finland).

Results

The amorphous cell construction required extra effort for polystyrene: the benzene rings tend to catenate during the building process. For this reason only one polymer chain was packed into a cell in order ensure that the simulation cell did not include any ring catenation. Usually, from the required amount of construction runs nearly half failed due to spearing of the rings. Isotactic chains were the most difficult to construct. Due to these difficulties we chose to carry out calculations for five cells of every tacticity, although averaging over so few configurations may not be adequate.

The initially constructed cells were very high in energy, and the cell was inhomogeneously filled. After the refinement procedure the cell was evenly filled and the corresponding five cells had total energies which were within 25 kcal/mol (see Table 1, which shows the total energy and its components for the refined cell that was built up using the probability of meso diads of 0.4). The Coulombic interactions are responsible for most of the variation in the total energy.

Analysis of the amorphous microstructures yields information on structural order: pair correlation functions

Table 4. Elastic Constants for Amorphous Polystyrene Calculated by Static Structure Deformation

probability of occurrence of meso diads	Young's modulus (GPa)	Poisson's ratio	bulk modulus (GPa)	shear modulus (GPa)
0.0	5.4 ± 0.6	0.30 ± 0.03	4.6 ± 0.6	2.1 ± 0.4
0.2	5.2 ± 0.3	0.30 ± 0.03	4.4 ± 0.5	2.1 ± 0.2
0.4	4.3 ± 0.2	0.32 ± 0.03	3.7 ± 0.5	1.6 ± 0.3
0.6	5.0 ± 0.7	0.32 ± 0.06	4.0 ± 0.6	1.7 ± 0.5
0.8	4.4 ± 0.8	0.30 ± 0.04	4.1 ± 0.6	1.8 ± 0.5
1.0	4.1 ± 0.7	0.34 ± 0.03	4.2 ± 0.2	1.5 ± 0.3
average	4.7 ± 0.6	0.31 ± 0.04	4.2 ± 0.5	1.8 ± 0.4
exptl value[21]	3.2–3.3	0.33		

$g(r)$ tell about the packing of the atoms in the cell. An example of correlation functions is shown in Figure 2. The figure is representing all the important and common features that can be observed in all calculated pair correlation functions. In the intramolecular part of the correlation function, the highest peaks can be found for carbon–carbon single and double bonds, respectively, and for carbon–hydrogen bonds. The distances between the atoms obey the limits of typical bond lengths. The intermolecular part shows that in the refined cell the distances between the atoms are well beyond the range of repulsive van der Waals interactions. Also, in the long-range region, the asymptotic value of unity is approached. When these two are combined to the total correlation function, it is observed that the function has a value of unity in the long-distance range; hence, there is no correlation of atoms which are separated by a distance longer than 5 Å.

The calculated cohesive energy densities were further utilized to calculate the solubility parameters. Values for the cohesive energy density and the solubility parameter are collected in Table 2. The computed values are slightly lower than the experimental values, this being in agreement with the common trend observed in previous calculations.

Table 5. Mechanical Properties for Various Polymers

polymer	Young's modulus		Poisson's ratio		bulk modulus		shear modulus	
	calcd value (GPa)	exptl value[21] (GPa)	calcd value (GPa)	exptl value (GPa)	calcd value (GPa)	expl value[21] (GPa)	calcd value (GPa)	exptl value[21] (GPa)
polypropylene[1-3]	2.990	2.650	0.35	0.37	3.250	3.340	1.11	0.97
	2.790		0.36		3.390		1.02	
polysulfone[7]	3.88 ± 1.51	2.6	0.24 ± 0.15		3.02 ± 1.48			
polycarbonate of 4,4′-isopropylidenediphenol[4-6]	5.60 ± 1.7	2.3–2.5	0.36 ± 0.06	0.42–0.43	6.7 ± 1.6	5.0–6.1		
polystyrene this work	3.5 ± 1.7	3.2–3.3	0.31 ± 0.04	0.33	4.2 ± 0.5		1.8 ± 0.4	

The tail correction of the nonbonded interaction energy ΔE_{tail} was −31.7 kcal/mol of structures.

According to the calculations, syndiotactic polystyrene has a higher value of cohesive energy density than the isotactic chain. No experimental evidence of this kind of behavior exists, but the physical background for this may arise from the interactions between polymer chains. For isotactic polystyrene chains, forces between neighboring benzene groups in the same chain are large and the tendency to intense interactions between different chains is less significant. On the contrary, syndiotactic polystyrene chains may intertwine more easily and can be enfolded with lesser effort,[11] this increasing the chain–chain interactions. Further explanation to this observation was sought by estimating the distribution of the free volume inside the simulation cell.

An example of a typical distribution of Voronoi polyhedra for carbon atoms is depicted in Figure 3, in this case for an atactic chain. Voronoi polyhedra are valuable representations for the free volume distribution in the sense that they demonstrate the local free volume. The total free amount of free volume may remain the same, although small changes in the local free volume content may occur. Also changes in the dominating polyhedron type may reflect differences in the local structure. All calculated Voronoi distributions show that the local free volume for carbon atoms changes as a function of tacticity. The changes are not remarkably large (see Table 3), but the carbons in isotactic polystyrene have slightly more local space than those in syndiotactic polystyrene (21% of carbons are surrounded by polyhedra which are larger than 25 Å^3 in isotactic polystyrene, while the percentage in syndiotactic polystyrene is only 15%). This supports the result that for syndiotactic polystyrene a larger value of cohesive energy density was predicted. Each polyhedron has more than 6 faces, and the most often encountered number of faces is 16. The surface area distributions have the highest peaks usually between 45 and 50 Å^2, showing no clear dependence on chain tacticity. The most probable value for the reduced surface/volume ratio, which is a measure for asphericity of the polyhedra, is 1.3 (the corresponding value for a sphere is 1.0). As a conclusion, no evidence of changes in the dominant polyhedron type was found as the tacticity of the chain changes.

Mechanical properties were estimated using both the static and dynamic approaches. In the static method the system ws distorted by three tensile and three shear deformations of magnitude ±0.0005, and after each deformation, the system was reminimized. The moduli obtained are depicted in Table 4. In Table 5 the values obtained are shown together with the results from previous calculations[1-7] in order to estimate the overall performance of the method.

In the dynamic method, a uniaxial tensile stress is applied stepwise along the x, y, and z directions. For each loading direction, constant stress dynamics is performed as a series up to 10 stages. At the end of each stage values for internal stress are recorded and thereafter the external stress is incremented by 0.05 GPa until strain exceeds 0.2. Recorded stress–strain data are averaged for all three directions, and the moduli are calculated using a least-squares fit to the averaged tensile stress versus tensile strain and to the average lateral strain versus tensile strain. Results are collected in Table 6.

Table 6. Elastic Constants for Amorphous Polystyrene Calculated by Stepwise Loading Molecular Dynamics

probability of occurrence of meso diads	Young's modulus (GPa)	Poisson's ratio	bulk modulus (GPa)	shear modulus (GPa)
0.0	2.2 ± 0.3	0.16 ± 0.05	1.1 ± 0.4	1.0 ± 0.2
0.2	2.0 ± 0.2	0.24 ± 0.06	1.4 ± 0.5	0.8 ± 0.1
0.4	2.2 ± 0.5	0.26 ± 0.02	1.6 ± 0.5	1.0 ± 0.2
0.6	2.5 ± 0.3	0.28 ± 0.08	1.8 ± 0.5	1.1 ± 0.2
0.8	2.5 ± 0.3	0.22 ± 0.07	1.6 ± 0.6	0.9 ± 0.3
1.0	2.5 ± 0.3	0.27 ± 0.02	1.6 ± 0.5	1.0 ± 0.3
average	2.3 ± 0.3	0.26 ± 0.05	1.5 ± 0.5	1.0 ± 0.2
exptl value[21]	3.2–3.3	0.33		

When the results obtained using two different approaches to calculate the mechanical properties are compared, the static method seems to yield the upper limit of values while the dynamic method gives the lower limit of prediction (see, for example, the results in Tables 4 and 6: Young's modulus calculated using the static structure deformation is 4.7 ± 0.6 GPa, and that estimated by stepwise loading molecular dynamics is 2.3 ± 0.3 GPa, these being compared to the experimental value of 3.2–3.3 GPa). To estimate the overall capability of the atom-based method to predict the mechanical properties of polystyrene, a combined average over both methods (also an average over all tacticities) for moduli is calculated (see Table 5). For example, Young's modulus has a value of 3.5 ± 0.5 GPa, which is in excellent agreement with the experimental value 3.2–3.3 GPa (atactic polystyrene).[21] On the other hand, comparison to experimental values is not so straightforward. Experimental values refer to atactic polystyrene, for which the probability of meso diads has been reported in the literature[22] to be 0.46. Second, the thermal and the processing history of the material under study as well as the direction of the applied load affect the resulting elastic constants in measurements. A detailed, reliable simulation of such a test is not easy.

We also wanted to examine the effect of chain tacticity on the calculated moduli. For the results obtained using the dynamic method, the moduli are nearly independent of the chain tacticity. Instead, the static method predicts variations in moduli when the probability of occurrence of meso diads is changed. For example, syndiotactic polystyrene is predicted to have a larger Young's modulus than isotactic polystyrene, which is in agreement with the larger cohesive energy density obtained for syndiotactic polystyrene.

The other aspect to consider is the computational cost of these two methods. The calculations carried out using the dynamic method required nearly twice as much CPU time as did the static calculations. Hence, because no essential improvement in values using the dynamic method is observed, the static method is still favored.

The ability to test the macroscopic behavior of polymeric, amorphous materials starting from their microscopic structure without any synthesis is a valuable tool. Hybrid calculation methods combining the simulations of amorphous and crystalline parts of polymeric material are needed to understand the behavior of a real polymeric material under mechanical load.

References and Notes

(1) Theodorou, D. N.; Suter, U. W. *Macromolecules* **1985**, *18*, 1467.
(2) Theodorou, D. N.; Suter, U. W. *Macromolecules* **1986**, *19*, 139.
(3) Theodorou, D. N.; Suter, U. W. *Macromolecules* **1986**, *19*, 379.
(4) Hutnik, M.; Argon, A. S.; Suter, U. W. *Macromolecules* **1991**, *24*, 5956.
(5) Hutnik, M.; Gentile, F. T.; Ludovice, P. J.; Suter, U. E. *Macromolecules* **1991**, *24*, 5956.
(6) Hutnik, M.; Argon, A. S.; Suter, U. W. *Macromolecules* **1991**, *24*, 5962.
(7) Fan, C. F.; Hsu, S. L. *Macromolecules* **1992**, *25*, 266.
(8) Ludovice, P. J.; Suter, U. W. Detailed Molecular Structure of a Polar Vinyl Polymer Glass. In *Computational Modeling of Polymers*; Bicerano, J., Ed.; Marcel Dekker, Inc.: New York, 1992.
(9) Li, Y.; Mattice, W. L. *Macromolecules* **1992**, *25*, 4942.
(10) Kim, E.-G.; Misra, S.; Mattice, W. L. *Macromolecules* **1993**, *26*, 3424.
(11) Raaska, T.; Sundholm, F.; Pietilä, L.-O. *Comput. Polym. Sci.* **1993**, *3*, 67.
(12) Brown, D.; Clarke, J. H. R. *Macromolecules* **1991**, *24*, 4073.
(13) Yoon, D. Y.; Sundararajan, P. R.; Flory, P. J. *Macromolecules* **1975**, *8*, 777.
(14) Allen, M. P.; Tildesley, D. J. *Computer Simulation of Liquids*; Clarendon Press: Oxford, U.K., 1987.
(15) Berendsen, H. J. C.; Postma, J. P. M.; van Gunsteren, W. F.; DiNola, A.; Haak, J. R. *J. Chem. Phys.* **1984**, *81*, 3684.
(16) INSIGHTII and DISCOVER, molecular modeling software, Biosym Technologies Inc., San Diego, 1992.
(17) Maple, J. R.; Dinur, U.; Hagler, A. T. *Proc. Natl. Acad. Sci.* **1988**, *85*, 5350.
(18) Maple, J. R.; Thatcher, T. S.; Dinur, U.; Hagler, A. T. *Chemical Design Automation News* **1990**, *5* (9).
(19) *DISCOVER User Guide*; part 1, version 2.9; Biosym Technologies Inc., San Diego, 1992.
(20) Maple, J. A.; Hwang, M. J.; Stockfisch, T. P.; Dinur, U.; Waldman, M.; Ewig, C. S.; Hagler, A. T. *J. Comput. Chem.*, accepted.
(21) Brandrup, J.; Immergut, E. H., Eds. *Handbook of Polymer Chemistry*; John Wiley & Sons, Inc.: New York, 1974.
(22) Kawamura, T.; Uryu, T.; Matsuzaki, K. *Macromol. Chem., Rapid Commun.* **1982**, *3*, 661.